The Cryosphere, 9, 753–766, 2015
www.the-cryosphere.net/9/753/2015/
doi:10.5194/tc-9-753-2015

The Cryosphere
Open Access

Tracing glacier changes in Austria from the Little Ice Age to the present using a lidar-based high-resolution glacier inventory in Austria

A. Fischer[1], B. Seiser[1], M. Stocker Waldhuber[1,2], C. Mitterer[1], and J. Abermann[3,*]

[1]Institute for Interdisciplinary Mountain Research, Austrian Academy of Sciences, Technikerstrasse 21a, 6020 Innsbruck, Austria
[2]Institut für Geowissenschaften und Geographie, Physische Geographie, Martin-Luther-Universität Halle-Wittenberg, Von-Seckendorff-Platz 4, 06120 Halle, Germany
[3]Commission for Geophysical Research, Austrian Academy of Sciences, Innsbruck, Austria
[*]now at: Asiaq – Greenland Survey, 3900 Nuuk, Greenland

Correspondence to: A. Fischer (andrea.fischer@oeaw.ac.at)

Received: 25 August 2014 – Published in The Cryosphere Discuss.: 15 October 2014
Revised: 23 March 2015 – Accepted: 27 March 2015 – Published: 27 April 2015

Abstract. Glacier inventories provide the basis for further studies on mass balance and volume change, relevant for local hydrological issues as well as for global calculation of sea level rise. In this study, a new Austrian glacier inventory has been compiled, updating data from 1969 (GI 1) and 1998 (GI 2) based on high-resolution lidar digital elevation models (DEMs) and orthophotos dating from 2004 to 2012 (GI 3). To expand the time series of digital glacier inventories in the past, the glacier outlines of the Little Ice Age maximum state (LIA) have been digitalized based on the lidar DEM and orthophotos. The resulting glacier area for GI 3 of $415.11 \pm 11.18\,km^2$ is 44 % of the LIA area. The annual relative area losses are $0.3\,\%\,yr^{-1}$ for the ∼ 119-year period GI LIA to GI 1 with one period with major glacier advances in the 1920s. From GI 1 to GI 2 (29 years, one advance period of variable length in the 1980s) glacier area decreased by $0.6\,\%\,yr^{-1}$ and from GI 2 to GI 3 (10 years, no advance period) by $1.2\,\%\,yr^{-1}$. Regional variability of the annual relative area loss is highest in the latest period, ranging from 0.3 to $6.19\,\%\,yr^{-1}$. The mean glacier size decreased from $0.69\,km^2$ (GI 1) to $0.46\,km^2$ (GI 3), with 47 % of the glaciers being smaller than $0.1\,km^2$ in GI 3 (22 %).

1 Introduction

The history of growth and decay of mountain glaciers affects society in the form of global changes in sea level and in the regional hydrological system as well as through glacier-related natural disasters. Apart from these direct impacts, the study of past glacier changes reveals information on palaeoglaciology and, together with other proxy data, palaeoclimatology and thus helps to compare current with previous climatic changes and their respective effects.

Estimating the current and future contribution of glacier mass budgets to sea level rise necessitates accurate information on the area, hypsography and ice thickness distribution of the world's glacier cover. In recent years the information available on global glacier cover has increased rapidly, with global glacier inventories compiled for the IPCC Report 2013 (Vaughan et al., 2013) complementing the world glacier inventories (WGMS and National Snow and Ice Data Center, 2012) and the one compiled by participants of the Global Land Ice Measurement from Space (GLIMS) initiative (Kargel et al., 2014). These global inventories serve as a basis for modelling current and future global changes in ice mass (e.g. Gardner et al., 2013; Marzeion et al., 2012; Radić and Hock, 2014). Based on the glacier inventories, ice volume has been modelled with different methods, partly as a basis for future sea level scenarios (Huss and Farinotti, 2012; Linsbauer et al., 2012; Radić et al., 2014; Grinsted, 2013).

On a regional scale, these glacier inventory data are used for calculating future scenarios of current local and regional hydrology and mass balance (Huss, 2012), as well as future glacier evolution. All this research is based on the most accurate mapping of glacier area and elevation at a particular point in time.

Satellite remote sensing is the most frequently applied method for large-scale derivation of glacier areas and outlines (Rott, 1977; Paul et al., 2010, 2011b, 2013). For direct monitoring of glacier recession over time, the linkage of the loss of volume and area to local climatic and ice dynamical changes, and the spatial extrapolation of local observations, time series of glacier inventories are needed. Time series of remote-sensing data naturally are limited by the availability of first satellite data (e.g. Rott, 1977), so that time series of glacier inventories have been limited to a length of several decades (Bolch et al., 2010). Longer time series (Nuth et al., 2013; Paul et al., 2011a; Andreassen et al., 2008) can only be compiled from additional data, such as topographic maps, with varying error characteristics (e.g. Haggren et al., 2007) and temporally and regionally varying availability.

Although the ice cover of the Alps is not a high portion of the world's ice reservoirs, scientific research on Alpine glaciers has a long history which is important in the context of climate change. Apart from the Randolph Glacier Inventory (RGI; Pfeffer et al., 2014; Ahrendt et al., 2012) and a pan-Alpine satellite-derived glacier inventory (Paul et al., 2011b), several national or regional glacier inventories are available for the Alps. For Italy, only regional data are available, for example for South Tyrol (Knoll and Kerschner, 2010) and the Aosta region (Diolaiuti et al., 2012). For the five German glaciers, time series of glacier areas have been compiled by Hagg et al. (2012). For the French Alps, a time series of three glacier inventories has been compiled showing the glacier states in 1967–1971, 1985–86 and 2006–2009 by Gardent et al. (2014). For Switzerland, several glacier inventories have been compiled from different sources. For the year 2000, a glacier inventory has been compiled from remote-sensing data (Kääb et al., 2002; Paul et al., 2004), for 1970 from aerial photography (Müller et al., 1976) and for 1850 the glacier inventory was reconstructed by Maisch et al. (1999). Elevation changes have been calculated between 1985 and 1999 for about 1050 glaciers (Paul and Haeberli, 2008) and recently by Fischer et al. (2014) for the period 1985–2010.

For the Austrian Alps, glacier inventories so far have been compiled and published for 1969 (Patzelt, 1980, 2013; Kuhn et al., 2008; GI 1) and 1998 (Lambrecht and Kuhn, 2007, Kuhn et al., 2008; GI 2) on the basis of orthophoto maps. Groß (1987) estimated glacier area changes between 1850, 1920 and 1969, mapping the extent of the Little Ice Age (LIA) and 1920 moraines from the orthophotos of the glacier inventory of 1969. As the Austrian federal authorities made lidar data available for the majority of Austria after years of very negative mass balances after 2000, these data have been used for the compilation of a new glacier inventory based on lidar digital elevation models (DEMs; Abermann et al., 2010). As the high-resolution data allow detailed mapping of LIA moraines, the unpublished maps of Groß (1987) have been used as the basis for an accurate mapping of the area and elevation of the LIA moraines, based on the lidar DEMs and the ice divides/glacier names used in the inventories GI 1 and GI 2.

The pilot study of Abermann et al. (2009) in the Ötztal Alps identified a pronounced decrease of glacier area, albeit differing for different size classes. The aim of this study was to update the existing Austrian glacier inventories 1969 (GI 1) and 1998 (GI 2) to a GI 3 and complement this as consistently as possible with a LIA inventory based on new geodata (Fig. 1) and the mappings of Groß (1987). The overarching research question answered by this study is the variability of Austrian glacier area changes and change rates by time, region, size class and elevation.

2 Data

2.1 Austrian glacier inventories

Lambrecht and Kuhn (2007) used othophotos between 1996 and 2002 to update the glacier inventory 1969 (GI 1), which they also digitized (Fig. 2). In the first, analogue, evaluation of the 1969 orthophotos the glacier area in 1969 was determined to be 541.7 km^2. The glacier areas have been delineated manually by Lambrecht and Kuhn (2007) and Kuhn et al. (2008) as recommended by UNESCO (1970); i.e. perennial snow patches directly attached to the glacier have been mapped as glacier area. The digital reanalysis of the inventory 1969 (GI 1) by Lambrecht and Kuhn (2007) found a total glacier area of 567 km^2, including also areas above the bergschrund. For GI 2 (Kuhn et al., 2013), Lambrecht and Kuhn (2007) used the same definition. A number of different flight campaigns were necessary to acquire cloud-free orthophotos with a minimum snow cover. Therefore, GI 2 dates from 1996 to 2002, but the main part of the glaciers were covered during the years 1997 (43.5 % of the total area) and 1998 (38.5 % of the total area). Lambrecht and Kuhn (2007) estimated the effect of compiling the glacier inventory from data sources of different years by calculating an area for the year 1998. The temporal homogenization of glacier area was done by upscaling or downscaling the recorded inventory area in specific altitude bands with a degree-day method to the year 1998. The difference between the recorded area and the area calculated for the year 1998 was only 1.2 km^2. They found a glacier area of 470.9 km^2 for the summed areas of different dates, and 469.7 km^2 for a temporally homogenized area for the year 1998. All the orthophoto maps and glacier boundaries are published in a booklet (Kuhn et al, 2008), showing also the low amount of snow cover in the orthophotos. The maximum error of the glacier area is estimated to be ± 1.5 %

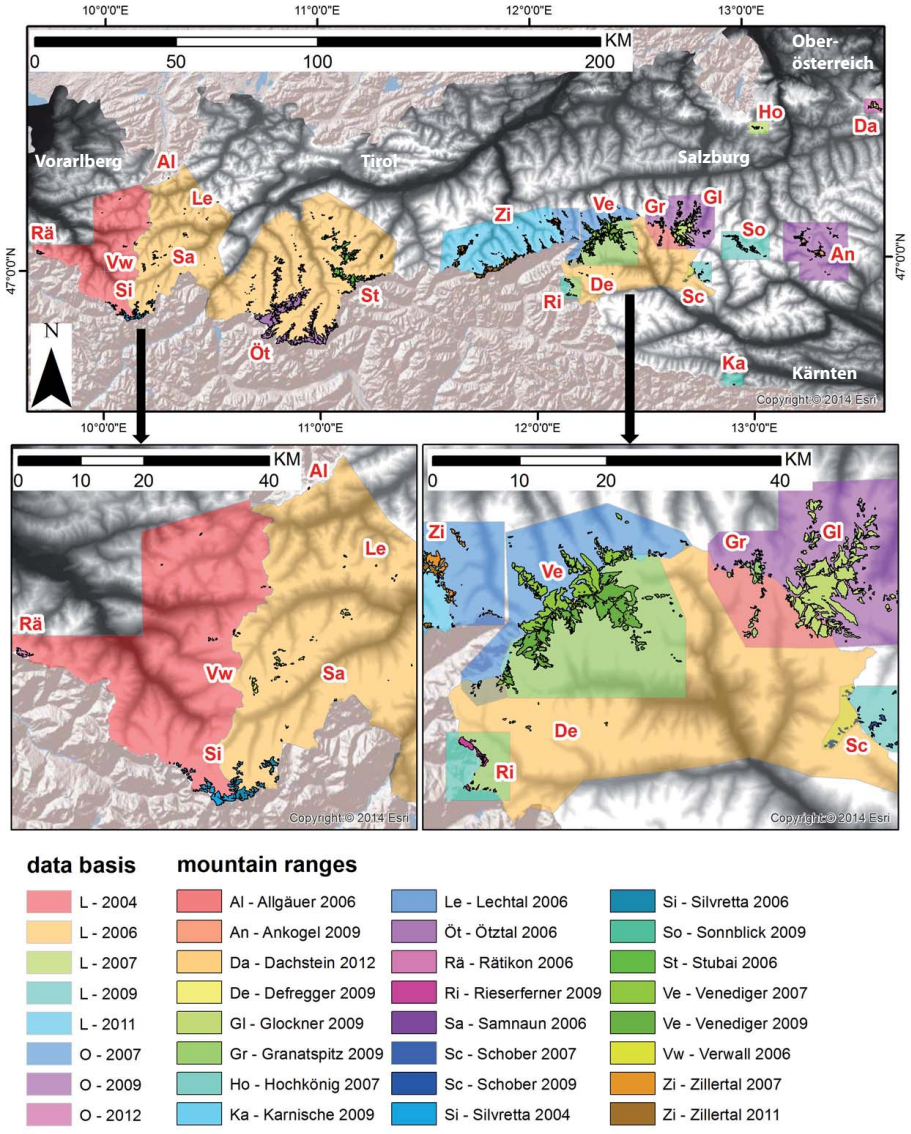

Figure 1. Austrian glaciers colour-coded by mountain ranges, with polygons showing data type and date used for deriving GI 3 and GI LIA (Mountain ranges and survey dates can also be found in Fischer et al. (2015).

(Lambrecht and Kuhn, 2007). About 3 % of the glacier area of 1969 has not been mapped, and several very small glaciers were still missing in GI 2. GI 1 and GI 2 comprise surface elevation models, with a vertical accuracy of ±1.9 m (Lambrecht and Kuhn, 2007).

2.2 Lidar data

Airborne laser scanning is a highly accurate method for the determination of surface elevation in high spatial resolution, allowing the mapping of geomorphologic features, such as moraines (Sailer et al., 2014). The recorded glacier elevation by lidar DEMs was compiled from a single date per glacier, although acquisition times of the DEMs vary from glacier to glacier. The sensors and requirements on point densities are listed in Table 1. Vertical and horizontal resolution also depends on slope and elevation; nominal mean values for flat areas are better than ±0.5 m (horizontal) and ±0.3 m (vertical) accuracy.

The point density in one grid cell of 1×1 m ranges from 0.25 to 1 point per square metre. The vertical accuracy depends on slope and surface roughness and ranges from a few centimetres to some decimetres in very steep terrain (Sailer et al., 2014). Lidar has a considerable advantage over photogrammetric DEMs where fresh snow or shading reduce vertical accuracy. As the high spatial resolution also reflects surface roughness, smooth ice-covered surfaces can be clearly distinguished from rough periglacial terrain. The flights were carried out during August and September in the

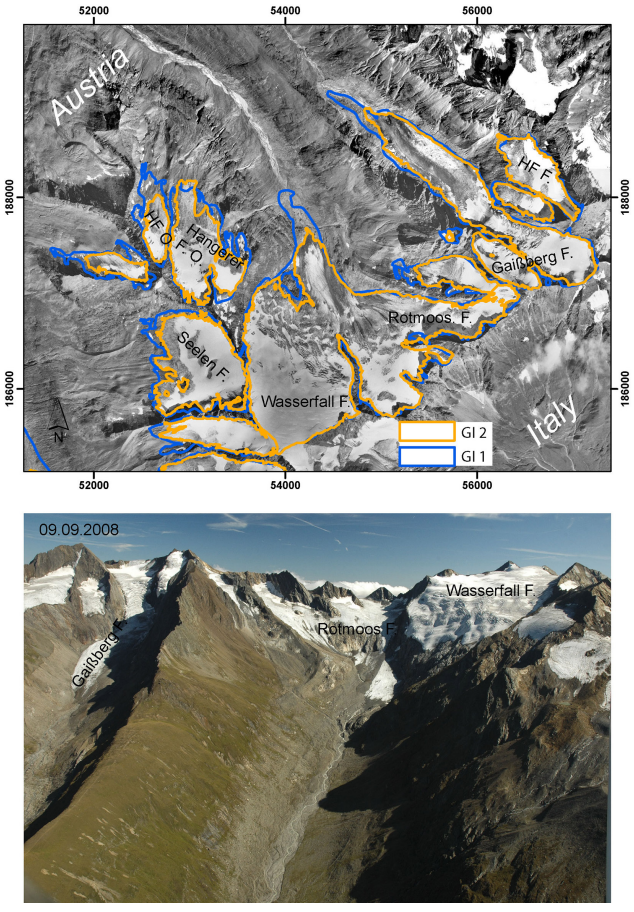

Figure 2. GI 1 and GI 2 glacier margins superimposed on a GI 2 orthophoto with an oblique photograph of the area in the Ötztal Alps. HF O: Hangerer Ferner Ost; HF F: Hochfirst Ferner.

years 2006 to 2012, when snow cover was minimal and the glacier margins snow-free.

2.3 Orthophotos

Orthophotos were used for the delineation of glacier margins where no lidar data were available. All orthophotos used are RGB true-colour orthophotos with a nominal resolution of 20 cm × 20 cm. Orthophotos from 2009 were used for the Ankogel–Hochalmspitze Group, Defregger Group, Glockner Group, Granatspitze Group, the western part of the Schober Group and the East Tyrolean part of the Venediger Group. Glacier margins in the eastern part of the Zillertal Alps and the northern part of the Venediger Group, located in Salzburg province, were determined using orthophotos from the year 2007. Orthophotos from 2012 were used for Dachstein Group.

3 Methods

3.1 Applied basic definitions

The compilation of the glacier inventory time series aims at monitoring glacier changes with time. Therefore, ice divides and specific definitions regarding what is considered a glacier were kept unchanged, although they could have been changed for the compiling of single inventories. To make the definitions used in this study clear, the definition of glaciers as well as glacier area and the separation by ice divides are specified here. Naturally, inventories which serve purposes other than compiling inventory time series will use other definitions, for example mapping changing ice divides instead of constant ones. The ice divides remain unchanged in all glacier inventories and are defined from the glacier surface in 1998. Although ice dynamics are likely to change between the inventories, leaving the position of the divides unchanged has the advantage that no area has shifted from one glacier to another. Mapping snow fields connected to the glacier as glacier area leads to an underestimate of glacier area changes if they increase in size and an overestimate if they melt.

The parent data set for this study is GI 1, so that the unique IDs in GI 1 were kept in later inventories. If a glacier had disintegrated in the inventory of 2006, one ID refers to polygons consisting of several parts of a formerly connected glacier area. For the disintegration of glaciers, the parent and child IDs as used in the GLIMS inventories (Raup et al., 2007; Raup and Khalsa, 2010) are a good solution. Going backwards in time, e.g. to where several parents of GI 1 are part of a larger LIA glacier, would consequently necessitate the definition of a grandparent or the division of the LIA glacier in different tributaries to allow a glacier-by-glacier comparison of area changes.

No size limit was applied for the mapping of glaciers in the 2006 inventory; i.e. glaciers whose area has decreased below a certain limit are still included in the updated inventory. This avoids an overestimate of the total loss of ice-covered area as a result of skipping small glaciers included in older inventories. The area of glaciers smaller than 0.01 km^2, which is often considered a minimum size for including glaciers in inventories, was also quantified.

3.2 Mapping the glacier extent in GI 3 from lidar

Abermann et al. (2010) demonstrated in a pilot study for the Ötztal Alps that lidar DEMs can be used with high accuracy for mapping glacier area. Figure 3 shows a lidar hillshade of glaciers in the Ötztal Alps dating from 2006 with orthofotos in VIS and CIR RGB from 2010 for comparison. The update of the glacier shapes from the inventory of 1998 was done combining hillshades with different illumination angles calculated from lidar DEMs (Fig. 4; for location of the subset see Fig. 3), analysing the surface elevation changes between the GI 2 and GI 3 inventories (Fig. 5; for location of

Table 1. Sensor and point densities.

	Sensor	Point density/m^2
Tyrol	ALTM 3100 and Gemini	0.25
Salzburg	Leica ALS-50, Optech ALTM-3100	1.00
Vorarlberg	ALTM 2050	2.50
Carinthia – Carnic Alps	Riegl LMS Q680i and Riegl LMS double-scan system	1.00
Carinthia – other	Leica ALS-50/83 and Optech Gemini	1.00

Table 2. Acquisition times of the glacier inventories with glacier areas for specific mountain ranges shown in Fig. 1; L means lidar ALS data and O means orthophoto.

Group	GI 2 year	GI 3 year	Data source	LIA km^2	GI 1 km^2	GI 2 km^2	GI 3 km^2
Allgäu Alps	1998	2006	L	0.29	0.20	0.09	0.07
Ankogel–Hochalmspitze Group	1998	2009	O	39.94	19.17	16.03	12.05
Dachstein Group	2002	2012	O	11.95	6.28	5.69	5.08
Defregger Group	1998	2009	O	2.01	0.70	0.43	0.30
Glockner Group	1998	2009	O	103.58	68.93	59.84	51.67
Granatspitze Group	1998	2009	O	20.08	9.76	7.52	5.48
Carnic Alps	1998	2009	L	0.29	0.20	0.18	0.09
Lechtaler Alps	1996	2004/2006	L	2.09	0.70	0.69	0.55
	1996	2006	L				0.36
	1996	2004	L				0.19
Ötztal Alps	1997	2006	L	280.35	178.32	151.16	137.58
Rätikon	1996	2004	L	3.12	2.19	1.65	1.61
Rieserferner Group	1998	2009	L	8.07	4.60	3.13	2.75
Salzburg Limestone Alps	2002	2007	L	5.68	2.47	1.68	1.16
Samnaun Group	2002	2006	L	0.59	0.20	0.08	0.07
Schober Group	1998	2007/2009	L/O	9.88	5.60	3.49	2.57
	1998	2007	L				0.96
	1998	2009	O				1.61
Silvretta Group	1996	2004/2006	L	41.27	23.96	18.97	18.48
		2006	L				9.86
		2004	L				8.62
Sonnblick Group	1998	2009	L	24.81	12.76	9.74	7.91
Stubai Alps	1997	2006	L	110.10	63.05	53.99	49.42
Venediger Group	1997	2007/2009	L/O	145.20	93.44	81.01	69.31
	1997	2007	O				29.85
	1997	2009	L				39.47
Verwall Group	2002	2004/2006	L	13.41	6.70	4.65	4.08
	2002	2006	L				3.66
	2002	2004	L				0.41
Zillertal Alps	1999	2007/2011	L/O	118.42	65.64	50.64	45.24
	1999	2007	O				4.73
	1999	2011	L				40.51
total area				941.13	564.88	470.67	415.47
% of LIA area				100.00	60.02	50.01	44.15

the subset see Fig. 3) and by comparison with orthophoto data, where available. The surface elevation change shows a maximum close to the position of the GI 3 glacier margin and should be zero outside the GI 2 glacier margin (apart from permafrost phenomena or mass movements). The resulting glacier boundaries are shown in Fig. 6. Abermann et al. (2010) quantify the accuracy of the areas derived by the lidar method to ± 1.5 % for glaciers larger than 1 km^2 and up to ± 5 % for smaller ones. The comparison with glacier margins measured by DGPS in the field for 118 points showed that

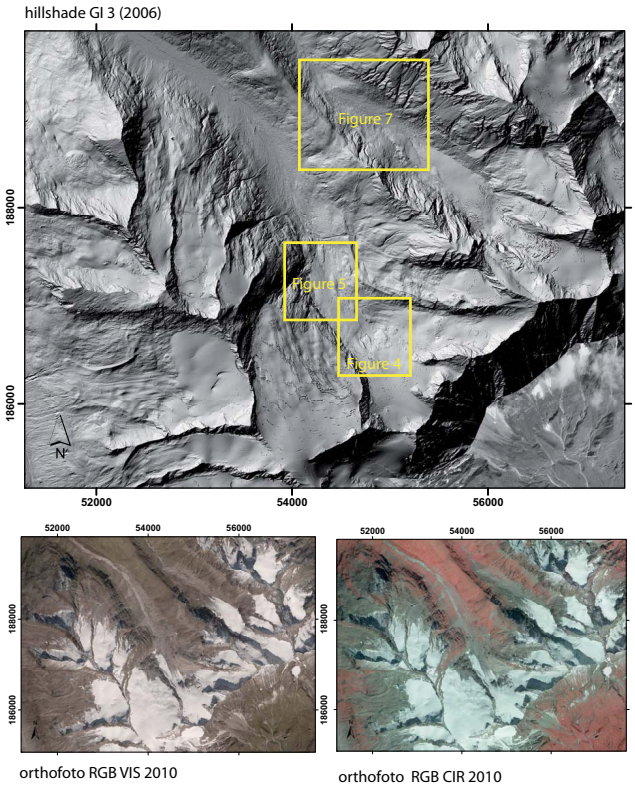

Figure 3. Example of an lidar hillshade (2006) of the same area as in Fig. 2 with VIS and CIR RGB orthophotos from 2010 for comparison. The inserts show the position of the subsets shown in Fig. 4 (lower right rectangle) and Fig. 5 (upper left rectangle).

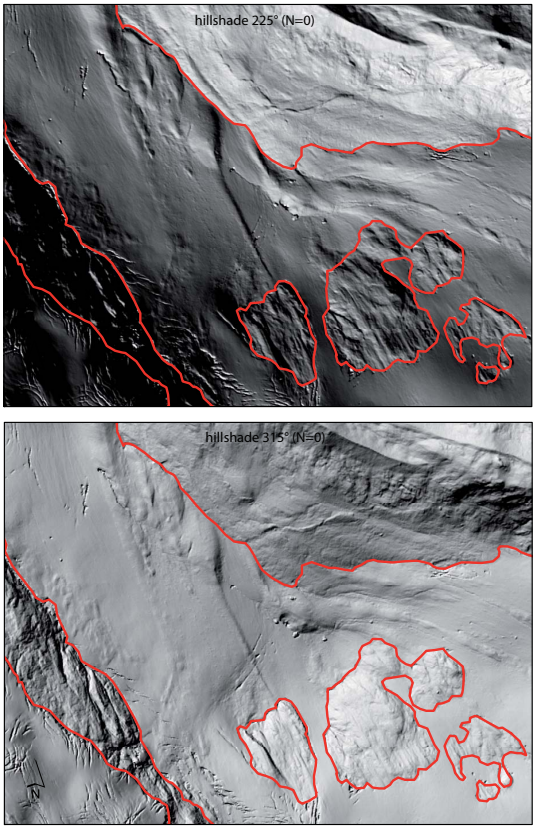

Figure 4. Hillshades from different view angles allow distinguishing smooth glacier surfaces from bedrock (position of the subset shown in Fig. 3).

95 % of these glacier margins derived from lidar were within an 8 m radius of the measured points and 85 % within a 4 m radius. Within this study, no experiment on quantifying differences between manual digitizing of different observers has been performed, as a number of studies with a high number of participants have already been carried out for VIS remote-sensing data (e.g. Paul et al., 2013).

3.3 Mapping the glacier extent in GI 3 from orthophotos

Where no lidar data were available (cf. Fig. 1, Table 2), the GI 2 glacier boundaries have been updated with orthophotos. As the nominal resolution of the orthophotos used for the manual delineation of the glacier boundaries is similar to GI 2, the estimated accuracy of the glacier area of ±1.5 % is considered to be valid also for GI 3.

3.4 Deriving the LIA extent

The LIA maximum extents were mapped based on previous mappings by Groß (1987) and Patzelt (1973), which were adapted to fit the moraine positions reorded in modern lidar DEMs and orthophotos. Groß (1987) and Patzelt (1973)

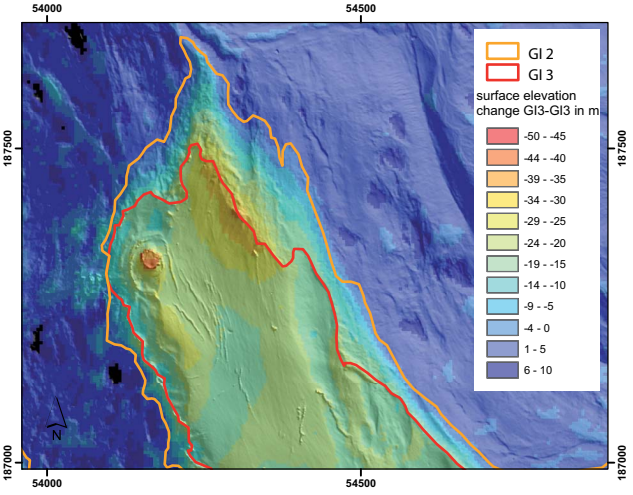

Figure 5. The elevation change between GI 2 and GI 3 superimposed on a hillshade shows that the elevation changes can help to delineate the actual (maximum elevation change) and previous (outer minimum of elevation change) position of the glacier margin (position of the subset shown in Fig. 3).

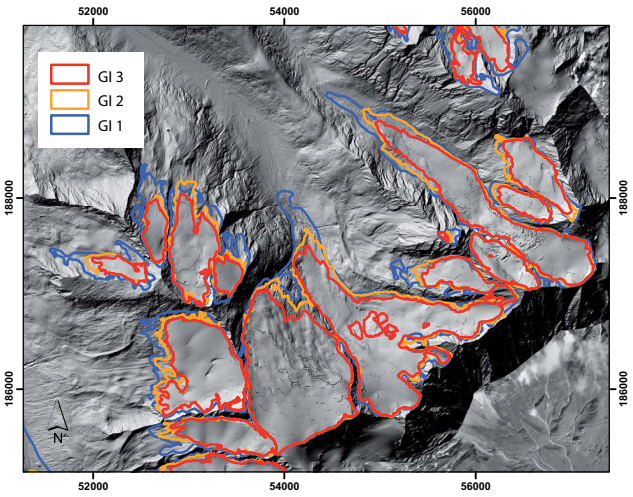

Figure 6. GI 3 glacier boundaries superimposed on lidar hillshade with GI 1 and GI 2 boundaries (same site as in Fig. 2).

mapped the LIA extents of 85 % of the Austrian glaciers based on field surveys and the maps and orthophotos of the 1969 glacier inventory. Their analogue glacier margin maps had been stored for several decades and suffered some distortion of the paper, so that the digitalization could not reproduce the position of the moraines according to the lidar DEMs. Therefore we decided to remap the LIA glacier areas, basically following the interpretation of Groß (1987) and Patzelt (1973), but remaining consistent with the digital data. Figure 7 shows the hillshades of the tongues of Gaißbergferner with pronounced LIA, 1920 and 1980 moraines, which are ice-cored in the orographic left side. The basic delineation of Groß (1987) was adapted to fit the LIA moraine in the lidar hillshade (Fig. 8).

Nevertheless, some smaller glaciers, which disappeared by 1969, might be missing in the LIA inventory. Groß (1987) accounted for these lost glaciers by adding 6.5 % to the LIA area, estimated from a comparison of historical maps and images as well as moraines. We decided to include this consideration in the discussion on uncertainties, although we think that this estimate is based on the best available evidence.

4 Results

4.1 Total glacier area

Austrian glaciers cover 941.1 km^2 (100 %) in GI LIA, 564.9 km^2 (60 %) in GI 1, 471.7 km^2 (50 %) in GI 2 and 415.1 km^2 (44 %) in GI 3 (Table 2). GI LIA was not corrected for glaciers which completely disappeared before GI 1, so that the area in this study is 4.4 km^2 smaller than the 945.5 km^2 found by Groß (1987). Only four glaciers have wasted down completely between GI 2 and GI 3. Shape files

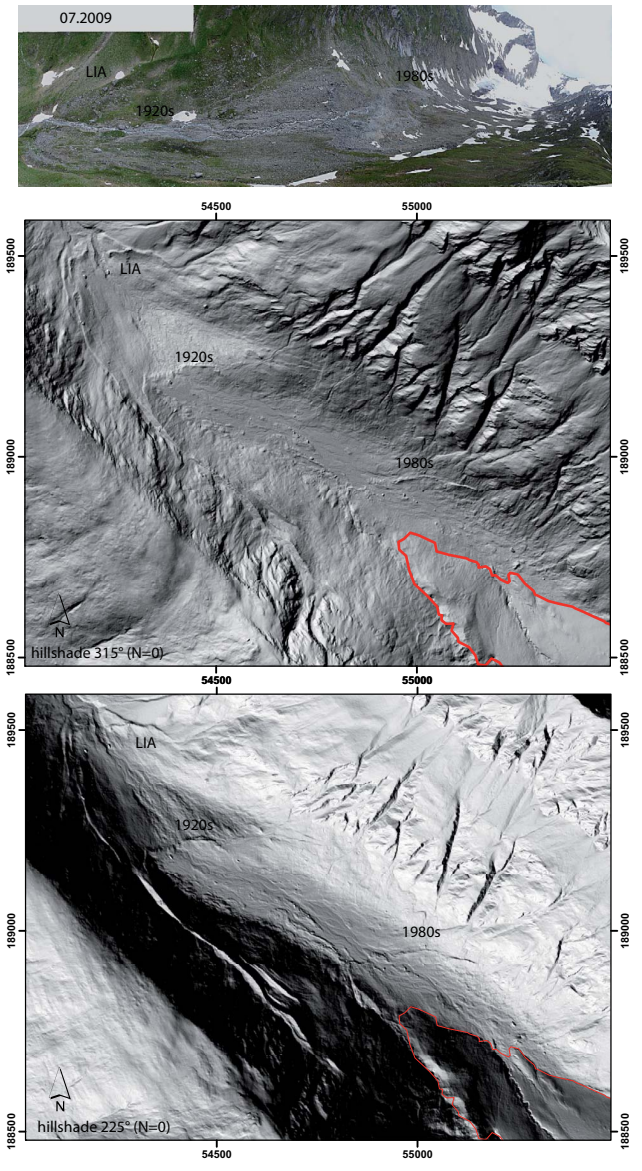

Figure 7. Periglacial area of Gaißbergferner with moraines dating from LIA, 1920 and 1980 (position of the subset: see Fig. 3).

of GI 3 can be downloaded via the Pangaea database (Fischer et al., 2015).

4.2 Absolute and relative changes of total area

The absolute loss of glacier area was 376 km^2 between GI LIA and GI 1, 94 km^2 between GI 1 and GI 2, and 55 km^2 between GI 2 and GI 3 (Table 2). Relative changes of the total area are 40 % (GI LIA to GI 1), 17 % (GI 1 to GI 2) and 12 % (GI 2 to GI 3). These numbers need a reference to the different period length for a comparison or interpretation, which is usually done by calculating relative changes per year. The glacier inventory periods can include subperiods with glacier advances and retreats, so that the calculated annual mean area

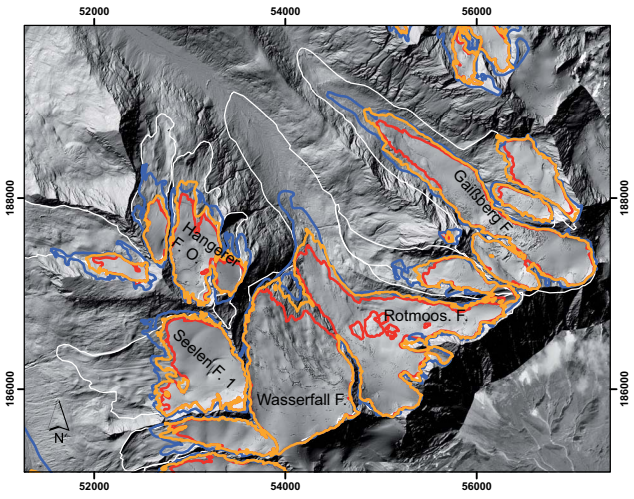

Figure 8. Resulting LIA glacier areas (white) with several modern glaciers contributing to the LIA Rotmoos Ferner and LIA Gaißbergferner (all glacier names: see Fig. 2).

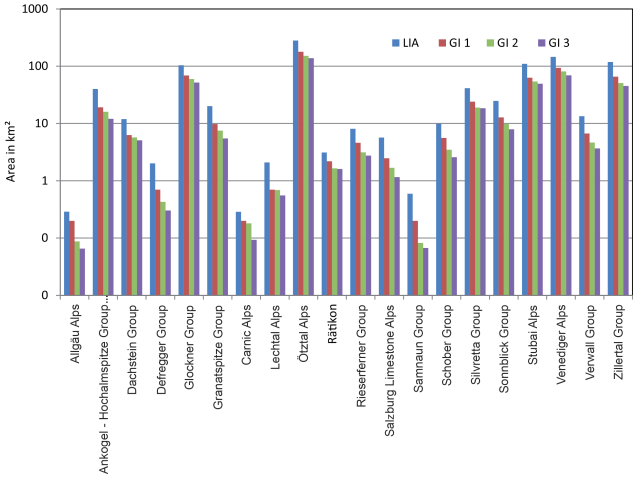

Figure 9. Glacier areas for specific mountain groups in GI LIA to GI 3.

change must be treated as an average value. The calculation of annual relative losses between GI LIA and GI 1 is based on the simplification that the LIA maximum occurred in 1850, so that the length of this period is 119 years. Then the relative area change per year is calculated to be 0.3 % yr^{-1}, including glacier advances around 1920 (Groß, 1987) and the temporal variability of the occurrence of LIA glacier maximum. The area-weighted mean of the number of years between GI 1 and GI 2 is 28.7, resulting in an annual relative change of total area of 0.6 % yr^{-1}. Within this period, a high portion of Austrian glaciers advanced (Fischer et al., 2013). The latest period, GI 2 to GI 3, showed a general glacier recession without significant advances, resulting in an annual relative area loss of 1.2 % yr^{-1} for the area-weighted period length of 9.9 years. Therefore, overall annual relative area losses in the

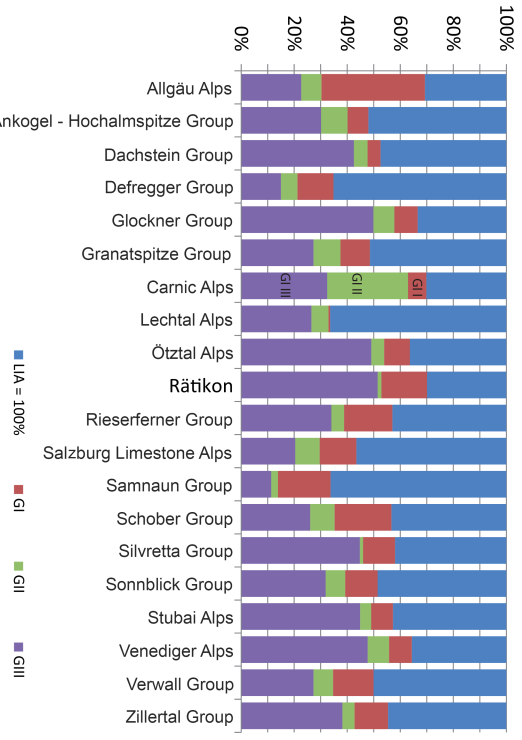

Figure 10. Area changes of specific mountain ranges in percentage of their LIA area.

latest period are twice as large as for GI 1 to GI 2 and 4 times as large as GI LIA to GI 1. Excluding retreat or advance periods for individual glaciers could show different annual area gain or loss rates. The numbers shown here represent the average annual area changes, without distinguishing between advance or retreat periods.

4.3 Results for specific mountain ranges

The absolute areas recorded for specific mountain ranges are shown in Fig. 9 and Table 2. Highest absolute glacier area decrease between GI 2 and GI 3 was observed in the Ötztal Alps (−13.9 km^2, 24 % of total area loss), the Venediger Group (−11.7 km^2, 20.9 % of total area loss), Stubai Alps (8.2 km^2, 4.5 % of total area loss) and Glockner Group (−8.17 km^2, 14.6 % of total area loss). These mountain ranges contribute 74.2 % of the total Austrian glacier area. Their contribution to the area loss, while only 60.4 %, is still lower than their share of glacier area. The contribution of the Ötztal Alps, Silvretta, Zillertal Alps and Stubai Alps to the total Austrian area loss has decreased between the LIA and today; the contribution of the Glockner Group and Venediger Group has increased by more than 4 % of the total area loss for each mountain range. The relative area loss since the LIA maximum differs between the specific groups: whereas only 11 % of the LIA area is left in the Samnaun Group, 51 to 45 % of the LIA area is still ice-covered in Rätikon, Ötztal Alps,

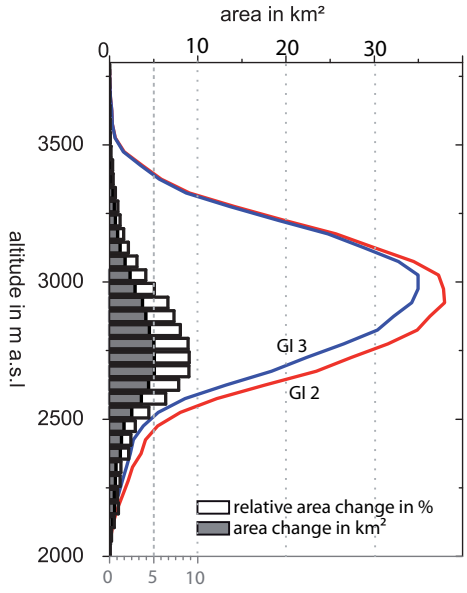

Figure 11. Altitudinal distribution of areas in GI 2 and GI 3 with absolute and relative area changes.

Venediger Group, Silvretta, Glockner Group and Stubai Alps (Fig. 10).

While the annual relative area losses in the first period vary between -0.3 and $-0.6\,\%\,yr^{-1}$, the regional variability of the relative annual area loss in the two latest periods is much higher the later (and shorter) the period (Table 3). As shown by Abermann et al. (2009), relative area changes differ for specific glacier sizes and periods, so that regional differences can also be interpreted as related to the specific glacier types and their geomorphology.

The highest annual relative area loss was observed in the Carnic Alps ($-4.5\,\%\,yr^{-1}$), Samnaun Group ($-5.6\,\%\,yr^{-1}$) and Verwall Group ($-5.9\,\%\,yr^{-1}$) for GI 2 to GI 3. These are groups with a high proportion of small glaciers.

4.4 Altitudinal variability of area changes

In GI 2, 88 % of the total area was located at elevations between 2600 and 3300 m a.s.l. (Fig. 11). In GI 3, the proportion of glacier area located at these elevations was still 87 %. The largest portion of the area is located at elevations between 2850 and 3300 m a.s.l. (41 % in GI 2 and 58 % in GI 3); 42 % of the area was located in regions above 3000 m in GI 2, decreasing to 39 % in GI 3. The area-weighted mean elevation of the glacier area is 2921 m a.s.l. in GI 2 and 2943 m a.s.l. in GI 3. As an approximation to a theoretical accumulation area ratio (AAR), 70 % of the glacier area is located above 3029 m a.s.l. in GI 2 and above 3046 m a.s.l. in GI 3.

The most severe absolute losses took place in altitudinal zones between 2650 and 2800 m a.s.l., with a maximum in the elevation zone 2700 to 2750 m a.s.l. Half of the area losses take place at altitudes between 2600 and 2900 m a.s.l. Therefore the main portion of the glacier-covered areas is stored in regions above the current strongest area losses.

4.5 Area changes for specific glacier sizes

The interpretation of the recorded glacier sizes has to take into account that not all glaciers which are mapped for newer inventories are part of the older inventories, as the total number of glaciers in Table 4 shows. Although some smaller glaciers are missing in GI 1, the number of glaciers smaller than 0.1 km^2 has been increasing, replacing the area class between 0.1 and 0.5 km^2 as the most frequent one. At the other end of the scale, 11 glaciers were part of the largest size class ($> 10\,km^2$) in GI 1 and only 8 were left in GI 3.

For GI 3, the glaciers in the largest size class of 5–10 km^2 cover 41 % of the area (Table 4). All other size classes range between 8 and 17 % of the total area, but glaciers of the smallest size class cover only 9 % of the total glacier area.

The percentage of area contributed by very small glaciers ($< 0.01\,km^2$) is small. In GI 1, one glacier covers 0.002 % (0.01 km^2) of the total glacier area. In GI 2, 16 very small glaciers cover 0.024 % (0.11 km^2) of the total glacier area. In GI 3, 26 very small glaciers contribute 0.033 % (0.14 km^2) of the total glacier area.

5 Discussion

The uncertainties of the derived glacier areas are estimated to be highest for the LIA inventory and to decrease with time to lowest for GI 3. For all glacier inventories, debris cover and perennial snow fields or fresh snow patches connected to the glacier are hard to identify, although including information on high-resolution elevation changes and including additional information from different points in time reduces this uncertainty (Abermann et al., 2010). The high-resolution data were only available for GI 3, so that the interpretation of debris and snow can still be regarded as an interpretational range of several percentage points for the area in GI 1 and 2. The nominal accuracy of the method (Abermann et al., 2010) results in an area uncertainty of $\pm 11.2\,km^2$, or $\pm 2.7\,\%$.

In the case of changing observers, differences in the interpretation of the glacier boundaries must be taken into account. Various studies exist on that topic, e.g. by Paul et al. (2013), who investigated the accuracy of different observers manually digitizing glacier outlines from high- (1 m) and medium-resolution (30 m) remote-sensing data and from automatic classification. They found high variabilities (up to 30 %) for debris-covered parts and about 5 % for clean ice parts. In contrast, in the presented study, all data have a spatial resolution of less than 5 m, GI 1 and GI 2 have been digitized manually by two observers and GI 3 followed their basic interpretation. The results of Paul et al. (2013) for chang-

Table 3. Relative and relative annual area changes.

Mountain group	GI 1–GI 2	GI 2–GI 3	LIA–GI 1	GI 2–GI 1	GI 3–GI 2	LIA–GI 1	GI 1–GI 2	GI 2–GI 3
	years	years	%	%	%	% yr^{-1}	% yr^{-1}	% yr^{-1}
Allgäu Alps	29	8	−31	−55	−22	−0.3	−1.9	−2.8
Ankogel–Hochalmspitze Group	29	11	−52	−16	−25	−0.4	−0.6	−2.3
Dachstein Group	33	10	−47	−9	−11	−0.4	−0.3	−1.1
Defregger Group	29	11	−65	−39	−30	−0.5	−1.3	−2.7
Glockner Group	29	11	−33	−13	−14	−0.3	−0.5	−1.2
Granatspitze Group	29	11	−51	−23	−27	−0.4	−0.8	−2.5
Carnic Alps	29	11	−31	−10	−50	−0.3	−0.3	−4.5
Lechtaler Alps	27	8, 10	−67	−1	−20	−0.6	−0.1	−2.2
Ötztal Alps	28	9	−36	−15	−23	−0.3	−0.5	−2.6
Rätikon	27	8	−30	−25	−25	−0.3	−0.9	−3.1
Rieserferner Group	29	11	−43	−32	−22	−0.4	−1.1	−2.0
Salzburg Limestone Alps	33	5	−57	−32	−18	−0.5	−1.0	−3.5
Samnaun Group	33	4	−66	−60	−22	−0.6	−1.8	−5.6
Schober Group	29	9, 11	−43	−38	−19	−0.4	−1.3	−1.8
Silvretta Group	27	8, 10	−42	−21	−25	−0.4	−0.8	−2.7
Sonnblick Group	29	11	−49	−24	−21	−0.4	−0.8	−1.9
Stubai Alps	28	9	−43	−14	−23	−0.4	−0.5	−2.6
Venediger Group	28	10, 12	−36	−13	−22	−0.3	−0.5	−2.0
Verwall Group	33	2, 4	−50	−31	−22	−0.4	−0.9	−5.9
Zillertal Alps	30	8, 12	−45	−23	−23	−0.4	−0.8	−2.0

Table 4. Absolute and relative number and areas of glaciers per size class.

Size classes (km^2)	< 0.1	0.1 to 0.5	0.5 to 1	1 to 5	5 to 10	> 10	Total
Number of glaciers							
in GI 1	177	401	116	99	11	5	809
in GI 2	401	343	92	79	7	3	925
in GI 3	450	307	77	77	8	2	921
Number of glaciers in %							
in GI 1	22	50	14	12	1	1	100
in GI 2	43	37	10	9	1	0	100
in GI 3	49	33	8	8	1	0	100
% of total area in class							
in GI 1	2	17	14	39	15	13	100
in GI 2	4	17	14	41	14	10	100
in GI 3	5	17	12	41	17	8	100
Area in class in km^2							
in GI 1	11.30	96.03	79.08	220.30	84.73	73.43	564.88
in GI 2	18.83	80.01	65.89	192.97	65.89	47.07	470.67
in GI 3	20.77	70.63	49.86	170.34	70.63	33.24	415.47

ing observers, resolutions or methods thus do not directly apply to this study.

The period length between GI 2 and GI 3 differs, as both glacier inventories show some temporal variability. The shortest period length was 2 years in the very small Verwall group (3.66 km^2, 0.88 % of the total glacier area). Only 1 % of the total area of GI 3 was recorded fewer than 5 years after GI 2, 1.3 % fewer than 8 years later and 5.3 % fewer than 9 years later. Gardent et al. (2014) and Paul et al. (2011a) found increasing change rates for short inventory periods, as they

Figure 12. Federal maps of the second and third federal survey (before and after the LIA maximum) show uncertainties in differentiation of snow, firn and glacier (arrows) but give some general impression on LIA glaciers.

found the uncertainties in the area assessment higher than the change rates. For the present study, the change rate in the shortest periods GI 2 to GI 3 (< 5 years) is −18 to −22 % of the GI 2 area and, thus, much larger than the mapping accuracy of 2.7 %. As the contribution of areas with short periods to the total area is small, the effect on the total area is also small.

Including seasonal or perennial snow fields attached to the glacier can introduce significant errors in calculating the glacier areas, affecting also area change rates when comparing inventories. The errors depend on the extent of the snow cover. As currently no operational method is available to identify snow-covered ground or perennial snow fields from VIS imagery, the only possibility to minimize these errors is to use remote-sensing data with minimum snow cover, which requires some additional information on the development of snow cover in the respective season from meteorological or mass balance time series. For future developments, radar imagery in L-band or tomographic radar as well as airborne ice thickness measurements could fill these gaps. As the firn and snow at the end of ablation season, when the minimum snow cover occurs and the perennial snow fields should be identified, still contains a high amount of liquid water, radar penetration depth decreases. An application to temperate glaciers as found in the Alps is therefore not feasible. Another important point is the often small extent of perennial snow fields and their location in small structures, such as gullies or troughs, which might be beyond the spatial resolution of low-frequency airborne or spaceborne radar systems.

For the interpretation of the LIA inventory, temporal and spatial indeterminacy has to be kept in mind. The temporal indeterminacy is caused by the asynchronous occurrence of the LIA maximum extent. In extreme cases the occurrence of the LIA maximum deviated several decades from the year 1850, which is often regarded as synonymous with the time of the LIA maximum.

The spatial indeterminacy varies between accumulation areas and glacier tongues: the moraines which confined the LIA glacier tongues give a good indication for the LIA glacier margins in most cases as they are clearly mapped in the lidar DEMs and changing vegetation is visible in the orthophotos. In some cases, lateral moraines standing proud for several decades eroded later, so that the LIA glacier surface will be interpreted not only as wider but also as lower than it actually was. In some cases, LIA moraines were subject to mass movements caused by fluvial or permafrost activities. In a very few cases, ice-cored moraines developed and moved from the original position. Altogether these uncertainties are small compared to the interpretational range at higher elevations, where no significant LIA moraines indicate the ice margins.

Moreover, historical documents and maps often show fresh or seasonal snow cover at higher elevations. For example the federal maps of 1816–1821 and 1869–1887 in Fig. 12 show surfaces where it is not clear if they are covered by snow, ice or firn. Therefore we cannot even be sure to have included all glaciers which existed during the LIA maximum. Groß (1987) calculated LIA maximum glacier areas of 945.50 km^2 without, and 1011.0 with, disappeared glaciers (i.e. 6.5 % disappeared glaciers). According to this estimate, 6.5 % of the LIA maximum area is possibly missing from our inventory. Taking this and a general mapping error of 3.5 % into account, we estimate the accuracy of the total ice cover for the LIA as ±10 %. Figure 12 illustrates that the maps of the third federal survey, together with other historical data, provide some information on the glacier area also in higher elevations.

In any investigation of large system changes, as between LIA and today, the definition of the term "glacier" is difficult, as it is not clear if it makes sense to compare one LIA glacier with the total area of its child glaciers with totally different geomorphology and dynamics, or if it would make more sense to split the LIA glacier into tributaries according to the present situation. In the present study, only the total glacier area in the mountain ranges has been compared.

Regarding the presented annual rates of area change, it has to be born in mind that all periods apart from GI 2 to GI 3 contain at least one period (around 1920 and in the 1980s) when the majority of glaciers advanced (Groß, 1987; Fischer et al., 2013). Thus a higher temporal resolution of inventories might result in different absolute and relative annual area change rates, as the length change rates, for example during the 1940s, have previously been in the same range as those after 2000.

The development of area change rates is similar to the ones found for the Aosta region by Diolaiuti et al. (2012), who arrived at $1.7\,\%\,\mathrm{yr}^{-1}$ for 1999 to 2005, and $0.8\,\%\,\mathrm{yr}^{-1}$ for 1975 to 1999. The maximum relative area changes in the period of the Austrian GI 2 to GI 3 exceed the ones summarized by Gardent et al. (2014). The periods for which area changes have been calculated for the French Alps by Gardent et al. (2014) are no exact match of the Austrian periods, but the total loss of 25.4 % of the glacier area between 1967 and 1971 and between 2006 and 2009 is similar to the Austrian Alps, despite the higher elevations of the French glaciers. A common finding is the high regional variability of the area changes. For the Swiss glaciers Maisch et al. (1999) found an annual relative area change of $-0.2\,\%\,\mathrm{yr}^{-1}$ for 1850 to 1973 and about $-1\,\%\,\mathrm{yr}^{-1}$ between 1973 and 1999. For the Alps Paul et al. (2004) reported an annual relative area change rate of $-1.3\,\%\,\mathrm{yr}^{-1}$ for the period 1985 to 1999. All the above-named periods differ in length and temporal occurrence, and the length and time of advance and retreat of glaciers vary. Therefore, even annual relative area change will not be fully comparable for the various inventories as they will also include regional and geomorphological variabilities.

The glacier inventories presented here show (i) high spatial resolution of the database used to derive the glacier outlines; (ii) inclusion of additional information, such as ground truth data, snow cover maps from mass balance surveys and time lapse cameras as well as meteorological data; (iii) minimal snow cover at the time of the flights; and (iv) consistent nomenclature and ice divides for all four inventories. Given legal and monetary limitations, it might be difficult or even impossible to acquire the data used for this inventory time series for all glaciers in the world. The acquisition of airborne data might be more expensive and time-consuming than buying satellite data. The high-resolution data used in this study are not available for a global inventory, nor is the high resolution beneficial for global studies, so that global inventories will naturally use satellite remote-sensing data. As the Alps often are used as an open space laboratory in glaciology, it nevertheless might make sense to compare results of global inventories with this regional inventory. The RGI Version 3.2, released 6 September 2013 and downloaded from http://www.glims.org/RGI/rgidl.html, contains 737 glaciers and a glacier area of $364\,\mathrm{km}^2$ for the year 2003. These numbers are lower than the ones recorded in the Austrian inventories (GI 2 before 2003 and GI 3 after 2003), although cross-border glaciers were not delimited for the comparison. This might be a matter of spatial scales, debris cover, shadows and different definitions applied, and it has no further implication.

6 Conclusions

This time series of glacier inventories presents a unique document of glacier area changes since the Little Ice Age. Total glacier area shrunk by 66 % between LIA maximum and GI 3, at increasing annual rates rising from $0.3\,\%\,\mathrm{yr}^{-1}$ (LIA–GI 1), to $0.6\,\%\,\mathrm{yr}^{-1}$ (GI 1–GI 2) to $1.2\,\%\,\mathrm{yr}^{-1}$ (GI 2–GI 3). During parts of the first two periods, some of the Austrian glaciers advanced, so that the latest period is the only one without glacier advances. The area changes vary for different mountain ranges and periods, with highest annual relative losses in the latest period (GI 2–GI 3) for the small ranges: Verwall Group ($-5.9\,\%\,\mathrm{yr}^{-1}$), Samnaun Group ($-5.6\,\%\,\mathrm{yr}^{-1}$) and Carnic Alps ($-4.5\,\%\,\mathrm{yr}^{-1}$). Nevertheless, for some of the largest glacier regions, like the Stubai Alps, Ötztal Alps and Silvretta Group, as well as for the small Rätikon, annual relative changes, even for the latest period, are smaller than $1\,\%\,\mathrm{yr}^{-1}$. Although the relative annual losses have generally increased since the LIA, some groups, for example the Silvretta Group and Rätikon, exhibit a decrease in the latest period. The only glacier in Salzburg Limestone Alps region, Übergossene Alm, is currently disintegrating with annual relative area losses of 6.2 % and will thus likely vanish in the near future. The area-weighted mean elevation increased from 2921 m a.s.l. in GI 2 to 2943 m a.s.l. in GI 3, with highest absolute area losses taking place in elevations between 2700 and 2750 m a.s.l. The number of glaciers in the smallest size class ($< 0.1\,\mathrm{km}^{-2}$) increased between GI 1 and GI 3, whilst the number of glaciers in the largest size class ($> 10\,\mathrm{km}^2$) decreased. The 10 glaciers in the two largest size classes still cover 25 % of the total glacier area. In GI 3, 49 % of the glaciers are in the smallest size class, but they cover only 5 % of the total glacier area.

For deriving a statistics for specific glaciers, a discussion of the implications of disintegration of glacier tributaries is needed, including more data from various climate regions. We encourage the use of the presented data basis for further studies and investigations of glacier response to climate change.

Acknowledgements. This study was supported by the federal governments of Vorarlberg, Tyrol, Salzburg, Upper Austria and Carinthia by providing lidar data. The Hydrographical Survey of the Federal Government of Salzburg supported the mapping of glaciers in Salzburg. For the province of Tyrol, the mapping of the LIA glaciers was supported by the Interreg 3P CLIM project. We are grateful for the contributions of Ingrid Meran and Markus Goller, who supported the project in their bachelor theses. Bernhard Hynek from ZAMG provided the glacier margins of the glaciers in the Goldberg Group. We thank Gernot Patzelt and Günther Groß for their helpful comments, and the reviewers Mauri Pelto, Siri Jodha Khalsa and Frank Paul for their suggestions which helped to thoroughly revise the manuscript.

Edited by: C. R. Stokes

References

Abermann, J., Lambrecht, A., Fischer, A., and Kuhn, M.: Quantifying changes and trends in glacier area and volume in the Austrian Ötztal Alps (1969-1997-2006), The Cryosphere 3, 205–215, doi:10.5194/tc-3-205-2009, 2009.

Abermann, J., Fischer, A., Lambrecht, A., and Geist, T.: On the potential of very high-resolution repeat DEMs in glacial and periglacial environments, The Cryosphere, 4, 53–65, doi:10.5194/tc-4-53-2010, 2010.

Andreassen, L. M., Paul, F., Kääb, A., and Hausberg, J. E.: Landsat-derived glacier inventory for Jotunheimen, Norway, and deduced glacier changes since the 1930s, The Cryosphere, 2, 131–145, doi:10.5194/tc-2-131-2008, 2008.

Arendt, A., Bolch, T., Cogley, J.G., Gardner, A., Hagen, J.-O., Hock, R., Kaser, G., Pfeffer, W. T., Moholdt, G., Paul, F. , Radić, V., Andreassen, L., Bajracharya, S., Barrand, N., Beedle, M., Berthier, E., Bhambri, R., Bliss, A., Brown, I., Burgess, D., Burgess, E., Cawkwell, F. , Chinn, T. , Copland, L., Davies, B., De Angelis, H., Dolgova, E., Filbert, K. ,R. Forester, R., Fountain, A., Frey, H., Giffen, B., Glasser, N., Gurney, S., Hagg, W., Hall, D., Haritashya, U. K. , Hartmann, G., Helm, C., Herreid, S., Howat, I., Kapustin, G., Khromova, T., Kienholz, C., Köonig, M., Kohler, J., Kriegel, D. , Kutuzov, S., Lavrentiev, I. , LeBris, R., Lund, J. , Manley, W., Mayer, C., Miles, E., Li, X. , Menounos, B., Mercer, A. , Mölg, N., Mool, P. , Nosenko, G., Negrete, A., Nuth, C., Pettersson, R., Racoviteanu, A., Ranzi, R., Rastner, P., Rau, F., Raup, B., Rich, J., Rott, H., Schneider, C., Seliverstov, Y., Sharp, M., Sigursson, O., Stokes, C., Wheate, R., Winsvold, S., Wolken, G., Wyatt, F., and Zheltyhina, N.: Randolph Glacier Inventory– A Dataset of Global Glacier Outlines: Version3.2., Global Land Ice Measurements from Space, Boulder Colorado, USA, Digital Media, http://www.glims.org/RGI/rgi_dl.html2012 (last access: 15 July 2014), 2012.

Bolch, T., Yao, T., Kang, S., Buchroithner, M. F., Scherer, D., Maussion, F., Huintjes, E., and Schneider, C.: A glacier inventory for the western Nyainqentanglha Range and the Nam Co Basin, Tibet, and glacier changes 1976–2009, The Cryosphere, 4, 419–433, doi:10.5194/tc-4-419-2010, 2010.

Diolaiuti, G. A., Bocchiola, D., Vagliasindi, M., D'Agata, C., and Smiraglia, C.: The 1975–2005 glacier changes in Aosta Valley (Italy) and the relations with climate evolution, Prog. Phys. Geogr., 36, 764–785, doi:10.1177/0309133312456413, 2012.

Fischer, A., Patzelt, G., and Kinzl, H.: Length changes of Austrian glaciers 1969–2013, Institut für Interdisziplinäre Gebirgsforschung der Österreichischen Akademie der Wissenschaften, Innsbruck, doi:10.1594/PANGAEA.82182, 2013.

Fischer, A et al.: The Austrian Glacier Inventories G 1 (1969), GI 2 (1998), GI 3 (2006), and GI LIA in ArcGIS (shapefile) format, http://doi.pangaea.de/10.1594/PANGAEA.844988 (DOI registration in progress), www.pangaea.de Supplement to: Fischer, Andrea; Seiser, Bernd; Stocker-Waldhuber, Martin; Mitterer, Christian; Abermann, Jakob (2014): Tracing glacial disintegration from the LIA to the present using a LIDAR-based hires glacier inventory, The Cryosphere Discussion, 8, 5195–5226, doi:10.5194/tcd-8-5195-2014, 2015.

Fischer, M., Huss, M., and Hoelzle, M.: Surface elevation and mass changes of all Swiss glaciers 1980–2010, The Cryosphere Discuss., 8, 4581–4617, doi:10.5194/tcd-8-4581-2014, 2014.

Gardent, M., Rabatel, A., Dedieu, J.-P., and Deline, P.: Multitemporal glacier inventory of the French Alps from the late 1960s to the late 2000s, Global Planet. Change, 120, 24–37, doi:10.1016/j.gloplacha.2014.05.004, 2014.

Gardner, A. S., Moholdt, G., Cogley, G., Wouters, B., Arendt, A. A., Wahr, J., Berthier, E., Hock, R., Pfeffer, W. T., Kaser, G., Ligtenberg, S. R. M., Bolch, T., Sharp, M. J., Hagen, J. O., van den Broeke, M. R., and Paul, F.: A Reconciled Estimate of Glacier Contributions to Sea Level Rise: 2003 to 2009, Science, 340, 852–857, doi:10.1126/science.1234532, 2013.

Grinsted, A.: An estimate of global glacier volume, The Cryosphere, 7, 141–151, doi:10.5194/tc-7-141-2013, 2013.

Groß, G.: Der Flächenverlust der Gletscher in Österreich 1850-1920-1969, Zeit. Gletscherk. Glazialgeol., 23, 131–141, 1987.

Hagg, W., Mayer, C., Mayr, E., and Heilig, A.: Climate and glacier fluctuations in the Bavarian Alps during the past 120 years, Erdkunde, 66, 121–142, 2012.

Haggren, H., Mayer, C., Nuikka, M., Rentsch, H., and Peipe, J.: Processing of old terrestrial photography for verifying the 1907 digital elevation model of Hochjochferner Glacier, Z. Gletscherk. Glazialgeol., 41, 29–53, 2007.

Huss, M. and Farinotti, D.: Distributed ice thickness and volume of all glaciers around the globe, J. Geophys. Res., 117, F04010, doi:10.1029/2012JF002523, 2012.

Huss, M.: Extrapolating glacier mass balance to the mountain-range scale: The European Alps 1900–2100, The Cryosphere, 6, 713–727, doi:10.5194/tc-6-713-2012, 2012.

Kääb, A., Paul, F., Maisch, M., Hoelzle, M., and Haeberli, W.: The new remote sensing derived Swiss glacier inventory: II. First results, Ann. Glaciol., 34, 362–366, 2002.

Kargel, J. S., Leonard, G. J., Bishop, M. P., Kaab, A., and Raup, B. (Eds.): Global Land Ice Measurements from Space (Springer-Praxis), in: an edited 33-chapter volume, Springer, Heidelberg, New York, Dodrecht, London, 876 p., 2014.

Knoll, C. and Kerschner, H.: A glacier inventory for South Tyrol, Italy, based on airborne laser-scanner data, Ann. Glaciol., 50, 46–52, 2010.

Kuhn, M., Lambrecht, A., Abermann, J., Patzelt, G., and Groß, G.: Die österreichischen Gletscher 1998 und 1969, Flächen und Volumenänderungen, Verlag der Österreichischen Akademie der Wissenschaften, Wien, 2008.

Kuhn, M., Lambrecht, A., and Abermann, J.: Austrian glacier inventory 1998, Alfred Wegener Institute, Bremerhaven, Germany, doi:10.1594/PANGAEA.809196, 2013.

Lambrecht, A. and Kuhn, M.: Glacier changes in the Austrian Alps during the last three decades, derived from the new Austrian glacier inventory, Ann. Glaciol., 46, 177–184, 2007.

Linsbauer, A., Paul, F., and Haeberli, W.: Modeling glacier thickness distribution and bed topography over entire mountain ranges with Glab-Top: Application of a fast and robust approach, J. Geophys. Res., 117, F03007, doi:10.1029/2011JF002313, 2012.

Maisch, M., Wipf, A., Denneler, B., Battaglia, J., and Benz, C.: Die Gletscher der Schweizer Alpen, Gletscherhochstand 1850 – Aktuelle Vergletscherung – Gletscherschwund-Szenarien 21. Jahrhundert, Zürich, Schlussbericht NFP31, vdf Hochschulverlag an der ETH Zürich, Zürich, 1999.

Marzeion, B., Jarosch, A. H., and Hofer, M.: Past and future sea-level change from the surface mass balance of glaciers, The Cryosphere, 6, 1295–1322, doi:10.5194/tc-6-1295-2012, 2012.

Müller, F., Caflisch, T., and Müller, G.: Firn und Eis der Schweizer Alpen, Gletscherinventar, Zürich, Geographisches Institut Publ. 57 and 57a, Eidgenössische Technische Hochschule, Zürich, 1976.

Nuth, C., Kohler, J., König, M., von Deschwanden, A., Hagen, J. O., Kääb, A., Moholdt, G., and Pettersson, R.: Decadal changes from a multi-temporal glacier inventory of Svalbard, The Cryosphere, 7, 1603–1621, doi:10.5194/tc-7-1603-2013, 2013.

Patzelt, G.: Die neuzeitlichen Gletscherschwankungen in der Venedigergruppe (Hohe Tauern, Ostalpen), Z. Gletscherk. Glazialgeol., 9, 5–57, 1973.

Patzelt, G.: The Austrian Glacier inventory: Status and first results, IAHS Publ., 126, 181–183, 1980.

Patzelt, G.: Austrian glacier inventory 1969, Alfred Wegener Institute in Bremerhaven, Germany, doi:10.1594/PANGAEA.807098, 2013.

Paul, F. and Haeberli, W.: Spatial variability of glacier elevation changes in the Swiss Alps obtained from two digital elevation models, Geophys. Res. Lett., 35, L21502, doi:10.1029/2008GL034718, 2008.

Paul, F., Kääb, A., Maisch, M., Kellenberger, T., and Haeberli, W.: Rapid disintegration of Alpine glaciers observed with satellite data, Geophys. Res. Lett., 31, L21402, doi:10.1029/2004GL020816, 2004.

Paul, F., Barry, R. G., Cogley, J. G., Frey, H., Haeberli, W., Ohmura, A., Ommanney, C. S. L., Raup, B., Rivera, A., and Zemp, M.: Guidelines for the compilation of glacier inventory data from digital sources, Ann. Glaciol., 50, 119–126, 2010.

Paul, F., Andreassen, L. M., and Winsvold, S. H.: A new glacier inventory for the Jostedalsbreen region, Norway, from Landsat TM scenes of 2006 and changes since 1966, Ann. Glaciol., 52, 153–162, 2011a.

Paul, F., Frey, H., and Le Bris, R.: A new glacier inventory for the European Alps from Landsat TM scenes of 2003: Challenges and results, Ann. Glaciol., 52, 144–152, 2011b.

Paul, F., Barrand, N., Berthier, E., Bolch, T., Casey, K., Frey, H., Joshi, S. P., Konovalov, V., Le Bris, R., Moelg, N., Nosenko, G., Nuth, C., Pope, A., Racoviteanu, A., Rastner, P., Raup, B., Scharrer, K., Steffen, S., and Winsvold, S.: On the accuracy of glacier outlines derived from remote sensing data, Ann. Glaciol., 53, 171–182, 2013.

Pfeffer, W. T., Arendt, A. A., Bliss, A., Bolch, T., Cogley, J. G., Gardner, A. S., Hagen, J. O., Hock, R., Kaser, G., Kienholz, C., Miles, E. S., Moholdt, G., Mölg, N., Paul, F., Radić, V., Rastner, P., Raup, B. H., Rich, J., Sharp, M. J., and the Randolph Consortium: The Randolph Glacier Inventory: a globally complete inventory of glaciers, J. Glaciol., 60, 537–551, doi:10.3189/2014JoG13J176, 2014.

Radić, V. R. and Hock, R.: Glaciers in the Earth's Hydrological Cycle: Assessments of Glacier Mass and Runoff Changes on Global and Regional Scales, Surv. Geophys., 35, 813–837, 2014.

Radić, V., Bliss, A., Beedlow, A.C., Hock, R., Miles E., and Cogley, J.G.: Regional and global projections of twenty-first century glacier mass changes in response to climate scenarios from global climate models, Clim. Dynam., 42, 37–58, 2014.

Raup, B. H. and Khalsa, S. J. S.: GLIMS analysis tutorial, 15 pp., available at: http://www.glims.org/MapsAndDocs/assets/GLIMS_AnalysisTutoriala4.pdf (last access: 16 April 2015), 2010.

Raup, B. H., Racoviteanu, A., Khalsa, S. J. S., Helm, C. Armstrong, R., and Arnaud, Y.: The GLIMS Geospatial Glacier Database: a new tool for studying glacier change, Global Planet. Change, 56, 101–110, 2007.

Rott, H.: Analyse der Schneeflächen auf Gletschern der Tiroler Zentralalpen aus Landsat-Bildern, Z. Gletscherk. Glazialgeol., 12/1, 1–28, 1977.

Sailer, R., Rutzinger, M., Rieg, L., and Wichmann, V.: Digital elevation models derived from airborne laser scanning point clouds: appropriate spatial resolutions for multi-temporal characterization and quantification of geomorphological processes, Earth Surf. Proc. Land., 39, 272–284, doi:10.1002/esp.3490, 2014.

UNESCO: Perennial ice and snow masses: a guide for compilation and assemblage of data for a world inventory, UNESCO/IASH Tech. Pap. Hydrol. 1, UNESCO/IASH, Paris, 1970.

Vaughan, D. G., Comiso, J. C., Allison, I., Carrasco, J., Kaser, G., Kwok, R., Mote, P., Murray, T., Paul, F., Ren, J., Rignot, E., Solomina, O., Steffen, K., and Zhang, T.,: Observations: Cryosphere, in: Climate Change 2013: The Physical Science Basis. Contribution of Working Group I to the Fifth Assessment Report of the Intergovernmental Panel on Climate Change, edited by: Stocker, T. F., Qin, D., Plattner, G.-K., Tignor, M., Allen, S. K., Boschung, J., Nauels, A., Xia, Y., Bex, V., and Midgley, P. M., Cambridge University Press, Cambridge, UK and New York, NY, USA, 2013.

WGMS and National Snow and Ice Data Center (comps.): World Glacier Inventory, National Snow and Ice Data Center, Boulder, Colorado, USA, doi:10.7265/N5/NSIDC-WGI-2012-02, 1999, updated 2012.